

HOSTED BY



ELSEVIER

Contents lists available at ScienceDirect

Engineering Science and Technology, an International Journal

journal homepage: www.elsevier.com/locate/jestch

Full Length Article

Correlation between vibration amplitude and tool wear in turning: Numerical and experimental analysis

Balla Srinivasa Prasad*, M. Prakash Babu

Mechanical Engineering, GIT, GITAM University, Visakhapatnam, India

ARTICLE INFO

Article history:

Received 28 October 2015

Revised 24 June 2016

Accepted 25 June 2016

Available online xxxxx

Keywords:

Vibration amplitude

Finite element modeling

Wear modeling

Cutting tools

Steel

Turning process

ABSTRACT

In this paper, a correlation between vibration amplitude and tool wear when in dry turning of AISI 4140 steel using uncoated carbide insert DNMA 432 is analyzed via experiments and finite element simulations. 3D Finite element simulations results are utilized to predict the evolution of cutting forces, vibration displacement amplitudes and tool wear in vibration induced turning. In the present paper, the primary concern is to find the relative vibration and tool wear with the variation of process parameters. These changes lead to accelerated tool wear and even breakage. The cutting forces in the feed direction are also predicted and compared with the experimental trends. A laser Doppler vibrometer is used to detect vibration amplitudes and the usage of Kistler 9272 dynamometer for recording the cutting forces during the cutting process is well demonstrated. A sincere effort is put to investigate the influence of spindle speed, feed rate, depth of cut on vibration amplitude and tool flank wear at different levels of workpiece hardness. Empirical models have been developed using second order polynomial equations for correlating the interaction and higher order influences of various process parameters. Analysis of variance (ANOVA) is carried out to identify the significant factors that are affecting the vibration amplitude and tool flank wear. Response surface methodology (RSM) is implemented to investigate the progression of flank wear and displacement amplitude based on experimental data. While measuring the displacement amplitude, *R*-square values for experimental and numerical methods are 98.6 and 97.8. Based on the *R*-square values of ANOVA it is found that the numerical values show good agreement with the experimental values and are helpful in estimating displacement amplitude. In the case of predicting the tool wear, *R*-square values were found to be 97.69 and 96.08, respectively for numerical and experimental measures while determining the tool wear. By taking *R*-square values into account, ANOVA confirms the close relation between experimental values and numerical values in evaluating the tool wear.

© 2016 The Authors. Publishing services by Elsevier B.V. on behalf of Karabuk University. This is an open access article under the CC BY-NC-ND license (<http://creativecommons.org/licenses/by-nc-nd/4.0/>).

1. Introduction

In turning operations, vibration is a frequent problem, which affects the result of machining, in particular, the tool wear. Vibration can be defined as an object being repeatedly displaced at a very high frequency [1]. In turning process, three types of mechanical vibrations are present. They are free, forced and self-excited vibrations. They occur due to lack of dynamic stiffness/rigidity of the machine tool system comprising tool, tool holder, workpiece and machine tool. Machining vibrations, also called as chatter, correspond to the relative movement between the workpiece and the cutting tool. These vibrations affect typical machining processes, such as turning, milling and drilling. Relative vibration amplitude

between the workpiece and cutting tool influences the tool life [2]. Cutting tool and tool holder shank are subjected to dynamic excitation due to the deformation of the work material during the cutting operation. The dynamic relative motion between the cutting tool and workpiece will affect the quality of the machining, in particular, the surface finish. Furthermore, the tool life is correlated with the amount of vibration [3]. In turning, the presence of tool vibration is a major factor which leads to poor surface finish, cutting tool damage, increase in tool wear and unacceptable noise [4]. Metal cutting processes can entail three different types of mechanical vibrations. They arise due to the lack of dynamic stiffness of one or several elements of the system comprising the machine tool, the tool holder, the cutting tool and the workpiece material [5]. Zhou et al. [6] presented a systematic approach based on Areal Power Spectral Density (APSD) method to identify the effect of relative vibratory motions between the tool and workpiece in diamond turning. The vibration amplitude, is the

* Corresponding author.

E-mail address: bsp.prasad@gmail.com (B.S. Prasad).

Peer review under responsibility of Karabuk University.

<http://dx.doi.org/10.1016/j.jestch.2016.06.011>

2215-0986/© 2016 The Authors. Publishing services by Elsevier B.V. on behalf of Karabuk University.

This is an open access article under the CC BY-NC-ND license (<http://creativecommons.org/licenses/by-nc-nd/4.0/>).

Please cite this article in press as: B.S. Prasad, M.P. Babu, Correlation between vibration amplitude and tool wear in turning: Numerical and experimental analysis, Eng. Sci. Tech., Int. J. (2016), <http://dx.doi.org/10.1016/j.jestch.2016.06.011>

Nomenclature

$Disp$	displacement due to vibration (microns)	d	depth of cut (mm)
N	rotational speed (rpm)	VB	flank wear (mm)
$Disp_{exp}$	experimental displacement value (microns)	ANOVA	analysis of variance (ANOVA)
$Disp_{num}$	numerical displacement value (microns)	RSM	response surface methodology
VB_{exp}	experimental flank wear (mm)	V_c	cutting speed (m/min)
VB_{num}	numerical flank wear (mm)	VB	flank wear (mm)
f	feed rate (mm/rev)		
H	workpiece hardness (Bhn)		

characteristic which describes the severity of the vibration, which can be quantified in several ways. In the present work, displacement is chosen to quantify the vibration amplitude during turning operation. Hence, the possibility of predicting the amount of the relative displacement amplitude and tool wear in machining processes is an interesting topic for industries. Most machining operations have two distinct motions: rotary motion and translation that is either straight or curvilinear. In operations such as milling and drilling, the tool is under motion and, thus, is the only component that vibrates [7]. In turning process, on the other hand, the workpiece has a rotary motion whereas the tool translates linearly. Both tool and workpiece vibrate in the process of material removal. However, throughout the years, researchers considered only tool vibration in cutting dynamics [8]. An exception to the previous i.e., workpiece deflection due to the exertion of 3D cutting forces and correlated dimensional errors has been recently considered [9,10]. Machining failures attributable to induced workpiece vibration that is often observed in the real world [11]. Workpiece vibration affects not only cutting instability but also product surface roughness and tool wear. Machine tool components are subjected to wide range of loads, due to the modification in cutter geometry, workpiece hardness, speed, feed and depth of cuts. Determination of machine tool vibration is highly critical and instrumental in increasing the quality of machining [12]. Most models developed for surface roughness [13] do not consider workpiece vibration, either. The cutting process actions applied to the machining system cause relative tool/workpiece displacements that can generate vibration. Consequently, instability in the cutting process can cause instability in the dynamic system of the machine tool resulting vibrations. Major directions in this field of research work aimed towards the advancement of productivity and cost-effectiveness. However, in automated manufacturing systems are focused on vibrations, detection of tool breakage and monitoring of cutting tool wear [14]. According to Paurobally et al. [15] chatter always indicates defects on the machined surface; vibration especially self-excited vibration is associated with the increased flank wear and machined surface roughness.

Chatter vibrations of the machining operation will damage the cutting tool if not addressed properly. Vibration displacement has a significant role in metal cutting. The displacement is a critical parameter for the predictive modeling of load distribution in cutting tool as well as for developing robust temperature prediction models [16]. Various other parameters may affect displacement amplitude while turning. However, there is still the lack of fundamental understanding of the phenomenon occurring at the tool-chip interfaces [17]. For these reasons, it is important for optimizing a machining process to be able to predict the amount of the tool wear. Antic et al. [18] presented the experimental investigation to study the influence of tool wear on the tool vibration and chip segmentation. This approach based on the assumption that a relationship exists between the high-frequency vibrations mea-

sured and tool wear degree. Antic et al. [19] demonstrated the procedure for acquiring high quality and timely information on vibration condition in real time with a particular emphasis on the module for acquisition and processing vibration signals. This investigation gives a clear understanding about the mechanism of the chip formation and segmentation type as well. They are used in the development of a system for identifying the tool wear. Zimmermann et al. [20] identified that workpiece and tool are subjected to severe mechanical and thermal loads while turning. The loads in turning can cause thermal expansions and mechanically induced deflections (vibrations) of the tool and the workpiece. They have presented the analysis of dry turning via experiments and 3D finite element simulations by using experimental results. Simulations with FEM in 3D case are performed recently, owing to advancements in re-meshing techniques in commercial FE codes, like Deform™ and Abaqus™, used in the present work [21,22].

Ozel et al. [23] investigated the effects of workpiece hardness, cutting edge geometry, cutting speed and feed rate on surface roughness and resultant forces in the finish hard turning of AISI H13 steel. Erol Zeren and Tuğrul Özel [24] demonstrated a 3D finite element method (FEM) modeling approach with arbitrary Lagrangian Eulerian (ALE) fully coupled thermal-stress analysis to simulate realistically high speed turning. Fazar et al. [25] used a finite element method (FEM) to simulate chip formation in the turning process and presented analytical as well as numerical analyses. This model is then used to predict machining attributes that are affected by the heat partition.

In conjunction with experiential investigations, tool wear prediction in machining is a constant preoccupation among researchers. Haddag et al. [26] presented a discussion on a phenomenological Usui's model to predict tool wear. According to Usui's model, tool wear is defined as a function of the tool-chip interface parameters, such as pressure, temperature and sliding velocity. The main advantage of such laws is the implantation ease.

Tugrul Ozel and Yigit Karpaz [27] presented a comparison of neural network models with regression models. Predictive neural network modeling is also extended to predict tool wear, and surface roughness patterns observed in finish hard turning processes [28]. Hence, to predict the factors that can affect the vibration amplitude and tool life a tool condition monitoring system is needed. An experimental evaluation of the tool wear parameters during turning process is a very expensive and time-consuming work, owing to the influence of many uncontrollable variables. There are several techniques for answering this problem like RSM [29] and ANNs. Feng and Wang [30] conducted testing and used regression analysis to develop a complete empirical model for traditional turning. Fang et al. [31] presented finite element simulations of machining for Ti-6Al-4V. In particular, the thermodynamic constitutive equation in FEA is applied for both workpiece material and tool material. The comparison between the experi-

mental and numerical cutting temperature and tool wear depth are presented and discussed. Researchers on tool life performed prediction models for optimization of process parameters. RSM technique is used for analyzing the influence of process parameters on tool wear and similar analyzes for different combinations are presented in [32–38]. Ding and He [39] developed a model of tool wear monitoring based on examined and analysis of the vibration signal in the time and frequency domains.

From the above literature, it is understood that most of the researchers are focused on determining the surface roughness and vibration characteristics in machining processes. In the present work, experimental tests have been carried to develop numerical models by using DOE that is capable of determining the vibration and surface roughness characteristics. A limited amount of information is found in the literature for correlating vibration amplitude and tool wear progression in face turning. It requires further studies to develop a correlation between displacement amplitude and flank wear during machining. Advanced process simulation techniques are essential to consider the influence of the tool wear and cutting conditions on the displacement amplitude, especially in the vibration induced machining processes. In this paper, an advanced FEM simulation technique is utilized to investigate the physical cutting process for predicting the displacement in the feed direction, temperature, and load variation during machining.

The objective of the present research is to apply RSM and ANOVA techniques to experimental, and FE simulated data. In the present study, a response surface methodology (RSM) has been used to analyze the effect of independent variables on the displacement amplitude and tool wear. The experiment is planned employing the design of experiments (DOE) technique. The variable parameters are rotational speed (N), feed rate (f), workpiece hardness (H) and depth of cut, and ANOVA was used to analyze the influence on flank wear (VB) and displacement due to vibration ($Disp$). The significance of the critical parameters (speed, feed, depth of cut) at different levels of workpiece hardness on the vibration amplitude and tool wear are determined using RSM.

2. Experimentation

Experiments are carried out on a PSG-124 lathe machine at constant cutting conditions. The machine has both auto feed and variable spindle speed capabilities. A Kistler® 9272 dynamometers with a multi-channel analyzer is used for acquisition of data on the cutting forces. A PolyTec 100V laser Doppler vibrometer with a data acquisition scheme is kept at a constant distance from the machining zone to measure the shift during the cutting process. The laser is concentrated along the rotating workpiece while machining is in progress. Oblique cutting parameters: Rake Angle ($^\circ$): -5 , Clearance Angle ($^\circ$): 5 , Flank face length (mm): 0.75 , Rake face length (mm): 1 . Machine: PSG Lathe, India. Specifications of lathe machine are as follows: Straight bed with single V having the length of 2.1 m, swing over the bed is 21 cm. Swing over the carriage is 14 cm and distance between centers is 96 cm. Motor capacity is 10 H.P., and it runs with a variable spindle speed range of 63 – 1250 rpm. Tool post of the machine is a square-headed type with a four jaw chuck. The turning operations are carried out with various cutting conditions to produces machined surfaces with varying flank wear values in correlation with displacement values.

Tool rejection criterion adopted for the present study is as follows. As per ISO 10816 standard for vibration severity, vibration displacements in the rotating object up to 20 microns do not have any effect on tool flank wear. Tool flank wear is found to be affected by the measured displacements in the range 20 – 60 microns. If the measured displacement value is beyond 60 μm , it

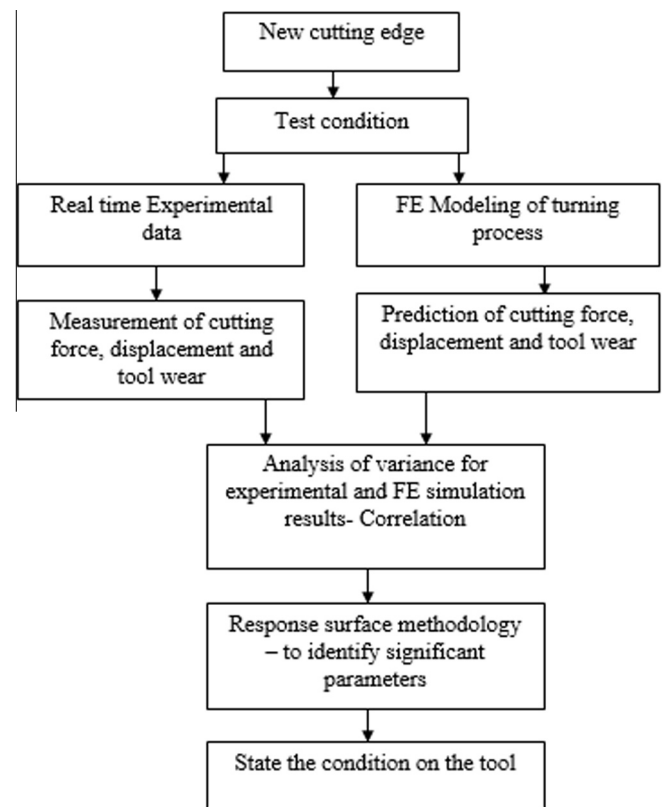


Fig. 1. Proposed methodology in the present study.

is not an acceptable as per ISO 10816. It is observed that in all conditions of experimental investigation, displacement values are found to be around 60 microns and flank wear $VB \leq 0.3$ mm. Fig. 1 presents the proposed methodology for the current study, and Fig. 2 shows the schematic representation of experimental setup.

As illustrated in Fig. 2, the distance between the vibration measuring equipment is maintained at 2 m from the experimental test rig. A laser from the laser Doppler vibrometer is allowed to focus on the rotating object. The way of mode conversion and reflection from the surface of workpiece can lead to interference pattern during the machining. This signal is amplified and fed to the FFT analyzer which is connected to a computer for analysis. Vibration signal analysis is performed for experimental data. A time domain wave graph is converted into a frequency domain as a spectrograph to obtain output in the specified range of frequency. The test setup developed in the present work is used for an acoustic-optic pulse generation while employing different cutting tool and workpiece materials combinations under various test conditions. In face turning, resonant vibration (chatter) occurs due to the forces enforced by the tool on the workpiece during machining. It causes the workpiece to vibrate at a natural frequency in which the smallest excitation makes the tremendous sense of vibration. The interaction between the tool and workpiece will keep on increases as the amplitude of vibration increases. A laser Doppler vibrometer (PDV-100) with amplifier (VIB-E-220 DAQ) is used to measure vibration amplitude in the feed direction. The wavelength forms from the vibration measurement output and is available in forms of amplitude, velocity, and displacement.

Vibrations can naturally occur in an engineering system and may be representative of its free and natural dynamic behavior. When the frequency of the forcing excitation coincides with that of the natural motion, the system will respond more vigorously

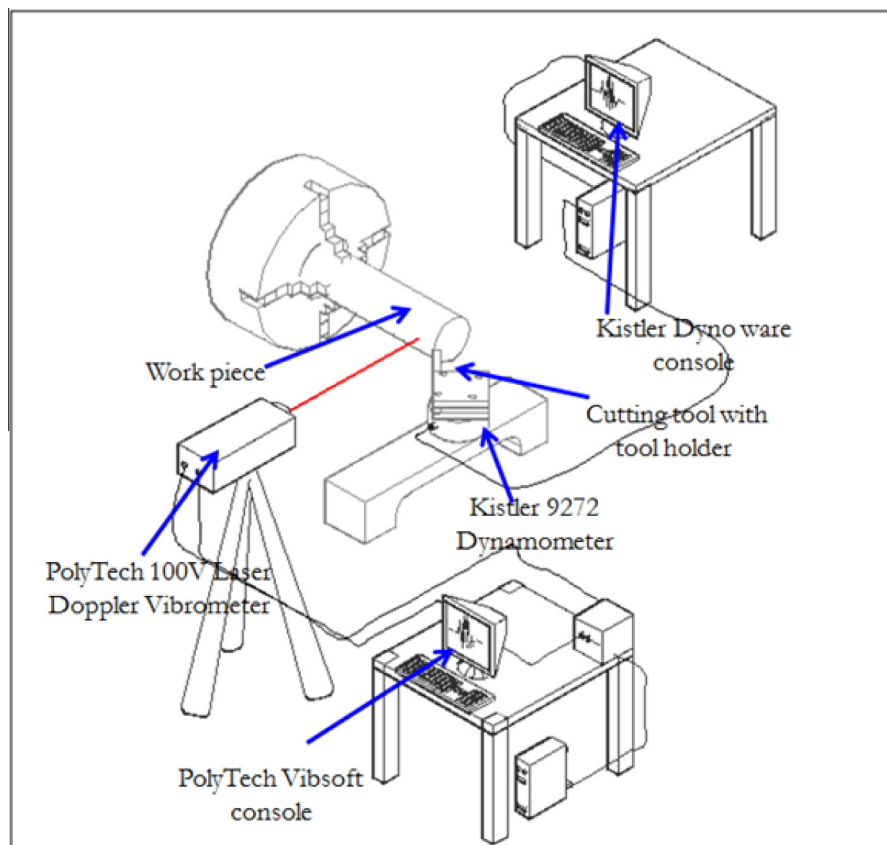


Fig. 2. Schematic representation of experimental setup used in the present study.

with increased amplitude. This condition is known as resonance, and the associated frequency is called the resonant frequency. The frequency ranges determined by the vibration response versus frequency can be developed by using the waveform of digital FFT analysis. The peak level is the indication of highest vibration produced during machining, and the peak amplitude of the turning process presented in this study. The peak value is particularly indicative of short duration shocks etc. In the present work, peak values are used to indicate maximum level that has occurred; not considering the account of the time history related to the vibration. Table 1 gives the test conditions chosen for experimental investigation for the present study.

When all instruments are ready, a turning process executed to perform face turning operation. The following procedural steps have been implemented to carry out the preliminary investigation.

Step 1. Each test started with a fresh cutting edge, and work-piece has been machined four times with every depth of cut,

Table 1
Oblique cutting parameters.

Oblique cutting parameters.		
Rake angle (°): -5, clearance angle (°): 5, flank face length (mm): 0.75, rake face length (mm): 1		
Cutting speed (<i>N</i> rpm)	Feed rate (mm/rev)	Depth of cut (mm)
538	0.08/0.4/0.8	0.4/0.8/1.2
836	0.08/0.4/0.8	0.4/0.8/1.2
1135	0.08/0.4/0.8	0.4/0.8/1.2
Work piece material AISI 4140 steel of size (Ø 80 × 150 mm)		
Carbide Tool Properties: DNMA432 (uncoated, WC as base material), Tool holder: DDJNR.		

and this process continued up to 36 passes of cut. At the end of every 4th pass of the cut, machining is stopped for measuring the tool wear.

Step 2. Vibration signals measured during the machining.

Step 3. Modify the cutting parameters as per new test condition and load the machine with a new workpiece. Repeat the step 1 and 2.

Step 4. For remaining test condition also, the same procedure has been implemented.

2.1. Effect of displacement amplitude on tool wear

Vibration raw signals are gathered using an LDV and plotted the vibration amplitude against time domain. This form of representation is called waveform graph. Waveform graph gives the percentage of vibration amplitude only for a particular time domain data. It is very difficult or often impossible to quantify the vibration levels with the help of waveform graph. Hence, waveform graphs are intentionally ignored from the results and discussions.

Moreover, direct the explicit time series analysis is usually incapable of isolating defect-scattered information appropriately from noise in different frequency bands. Therefore, time domain signal must be converted into converted to frequency domain as spectrum graphs by using a fast Fourier transform (FFT). Fast Fourier transform is utilized to determine the vibration parameter, i.e., displacement (microns) in the frequency domain for analysis of the vibration signal. Fig. 3 gives the frequency domain graph at three critical stages of the experiment. The spectrum graph presented in Fig. 3 provides more information about machining process than the waveform graph. The displacement value determined after vibration signal analysis used as a parameter for assessing the cutting tool condition. Therefore, vibration displacement plays a sig-

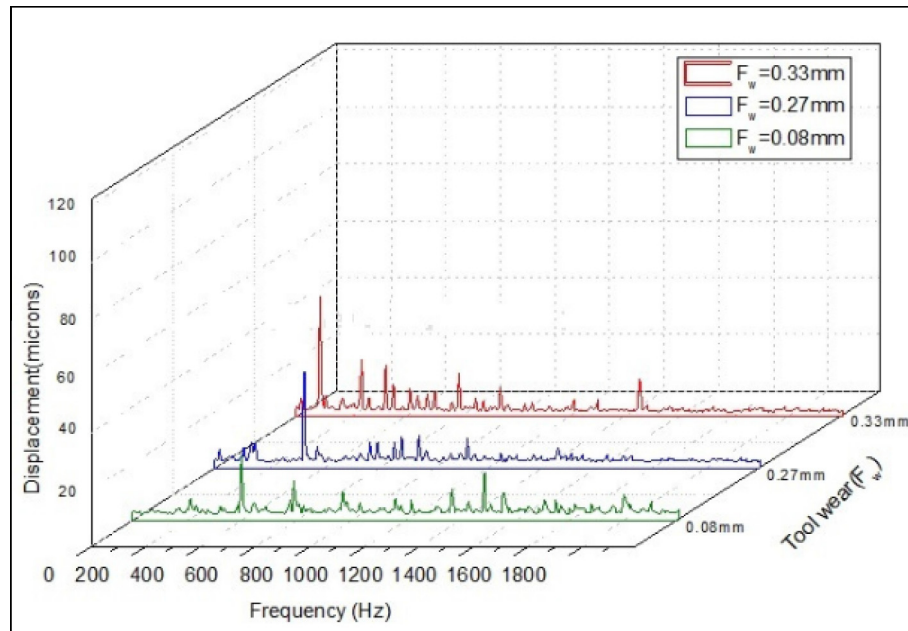


Fig. 3. Frequency spectra for vibration signals at various test conditions.

nificant role in estimating the tool wear. A displacement value beyond $60\ \mu\text{m}$ is not an acceptable as per ISO 10816. From the results Table 1, it is clear that in all conditions, i.e., TC 1-1 to TC 1-9 displacement values are observed to be less than 60 microns. Vibration signature data of different test conditions shown in Fig. 3.

In face turning, the stiffness of the workpiece increases as the length of the workpiece decreases and the corresponding increase in vibration amplitude is recorded. This variation in vibration levels at different test conditions shown in Fig. 3. In Fig. 3, a further increase in vibration amplitude is found in comparison with other two test conditions. In this connection, Friction increases between the workpiece and cutting tool that is due to increase in tool wear [40]. According to Lim [41], force and acceleration signals in the feed direction are significant, signals in the other directions not revealing any useful information. A strong correlation between tool flank wear and vibration is evident. After that, a second peak appears as the tool reaches and passes its wear limits, after which the friction decreases and vibration amplitude correspondingly drops and fail. Fig. 3 shows the impact of spindle speed on vibrations. Displacement amplitude of workpiece keeps on increasing the spindle speed. From the empirical model, it is clear evident that the vibration increases with the speed. There is a significant effect of vibrations when increasing or decreasing the feed rate. From Fig. 3, it is clear that vibration amplitude increases along with tool wear. Displacement amplitude in the feed direction is found to be acceptable as long as the depth of cut value is $0.5\ \text{mm}$ according to ISO 10816. Displacement amplitude is found to be affected by the depth of cut values of $0.8\ \text{mm}$ and $1.5\ \text{mm}$.

From results, it is observed that cutting speed, feed rate and depth of cut at different levels of workpiece hardness shows more influence on vibration amplitude (displacement) in throughout the experiment. In the present work, ANOVA method is used to investigate effects of factors (input parameters) on responses (output parameters). In experimental investigations, ANOVA is often employed before other statistical analysis. Then regression analysis is used which establishes a relation between independent variables (factors) and dependent variables (responses) were applied. Regression analysis was used to derive polynomial equations.

3. Three-dimensional finite element modeling and simulation of turning process

The three-dimensional model developed using Deform 3D v6.1, is reported in Fig. 4 that shows the cutting tool and workpiece with the growing chip. Cutting tool is assumed to be as rigid object meshed with more than 75,000 elements, and it is oriented to move along linear direction according to the cutting angles set in experimental test conditions. The workpiece, considered to be a rigid elasto-plastic object meshed with more than 30,000 elements and are fully constrained on the lower and lateral sides so that it cannot move. The friction is modeled considering a shear factor equal to 0.6. Adaptive re-meshing scheme optimizes the computational time and accurate prediction. The base of the workpiece remains constrained in all directions. The tool is subjected to move in Y direction at three different constant speeds and constrained against movements in X and Z directions. A commercial software Deform 3D with dynamic ALE modeling approach [31] is used to conduct the FEM simulation of face turning considering the tool edge geometry and remaining all the attributes implemented in the model. The chip formation is simulated via adaptive meshing and plastic flow of work material. Therefore, there is no chip separation criterion is needed.

In this approach, the elements are attached to the tool material, and the un-deformed tool is advanced towards the workpiece. Mechanical and thermal properties are necessary to develop the thermo-mechanical FEM simulation model of the machining system. Fig. 4 shows the FE simulation model consisting of boundary conditions, contact conditions between tool and workpiece.

3.1. Material flow properties

Material properties are essential inputs for an FEA simulation of a machining process. To represent the constitutive behavior of the cutting tool and workpiece material under specific cutting conditions, it is necessary to have an accurate and reliable flow stress model that is capable of representing hardening, strain rate hardening and thermal softening. The following Johnson–Cook material model used in machining simulation [42]. In this work, the

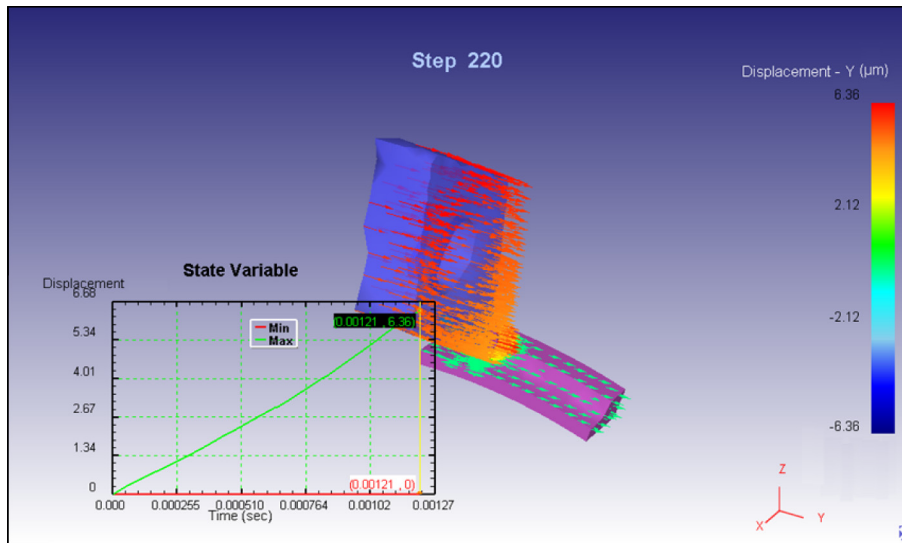


Fig. 4. Deformation in turning process (displacement due to vibration).

Johnson–Cook constitutive model was used to predict the post-yield behavior of AISI 4140 steel is given by Eq. (1) is used.

$$\bar{\sigma} = (A + B\bar{\epsilon}^n) \left[1 + C \ln \left(\frac{\dot{\bar{\epsilon}}}{\dot{\bar{\epsilon}}_0} \right) \right] \left[1 - \left(\frac{T - T_{room}}{T_{melt} - T_{room}} \right)^m \right] \quad (1)$$

where $\bar{\sigma}$, flow stress, $\dot{\bar{\epsilon}}$ is plastic strain rate, $\bar{\epsilon}$ is equivalent plastic strain, $\dot{\bar{\epsilon}}_0$ is reference strain rate, A is initial yield stress, B is hardening modulus, C is strain rate dependency coefficient, n is work hardening exponent, m is thermal softening coefficient, T is the process temperature, T_{melt} is the melting temperature of the workpiece and room T_{room} is the ambient temperature (35 °C). The Johnson–Cook model provides a good fit for the mechanical behavior of metals and it is numerically robust and can be used in FEA models. Many researchers used the Johnson–Cook model as constitutive equation in FEA modeling of orthogonal machining and Johnson–Cook parameters considered for the present work are shown in Table 2 along with boundary conditions in FE simulations.

Fig. 5(a) gave the meshed model of AISI 4140 steel and meshed model of the cutting insert presented in Fig. 5(b). Deform 3D software use for modeling and simulating the cutting process is capable of performing coupled thermo-mechanical transient analysis. As discussed in the literature, present research work is aimed at the 3D numerical prediction of tool wear using the knowledge acquired in 2D studies. Thus, to validate 3D numerical predictions for both flank and displacement owing to vibration, a series of experiments have been carried out in turning.

To estimate tool wear for the cutting tool and work material combination selected in the adopted cutting configuration, the

Table 2
Johnson cook parameters for workpiece and cutting tool [43].

Work piece/cutting tool	A (MPa)	B (MPa)	n	C	m
AISI 4140 [17]	806	614	0.618	0.0089	1
Uncoated carbide insert (WC-Co) [21]	0.003	8.0471	0.0003	0	0.179
Boundary condition					
Initial temperature	Shear friction factor	Heat transfer coefficient at the interface (N/s mm°C)			
25 °C	0.6	45			

phenomenological Usui’s wear law [44] is used. Interface pressure, sliding velocity, interface temperature, time increment and experimentally calibrated coefficients are the parameters for FE analysis.

3.2. Relationship of FE simulation results with experimental results

Fig. 6 presents the 3D finite element simulation results at different stages of the experiment. The objective of this section is to

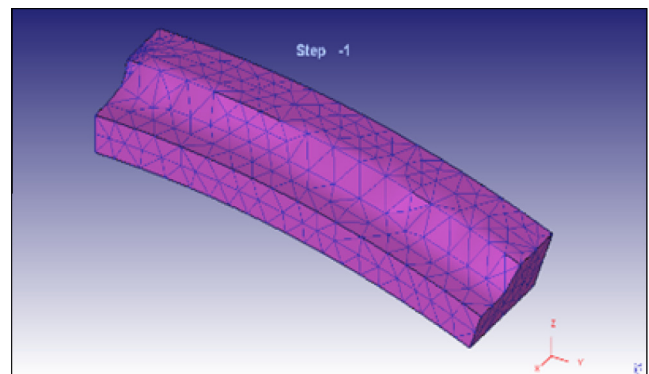


Fig. 5. (a) Modeling of 4140 workpiece. (b) Modeling of uncoated insert.

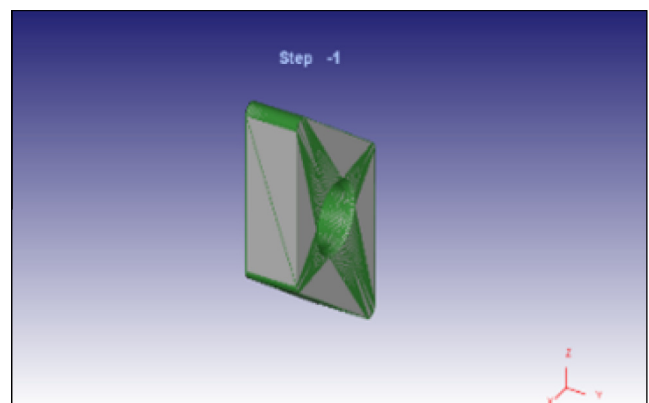


Fig. 5 (continued)

TC 1-1: Rotational speed 538 rpm, feed at 0.08mm/rev, depth of cut 0.4 mm)

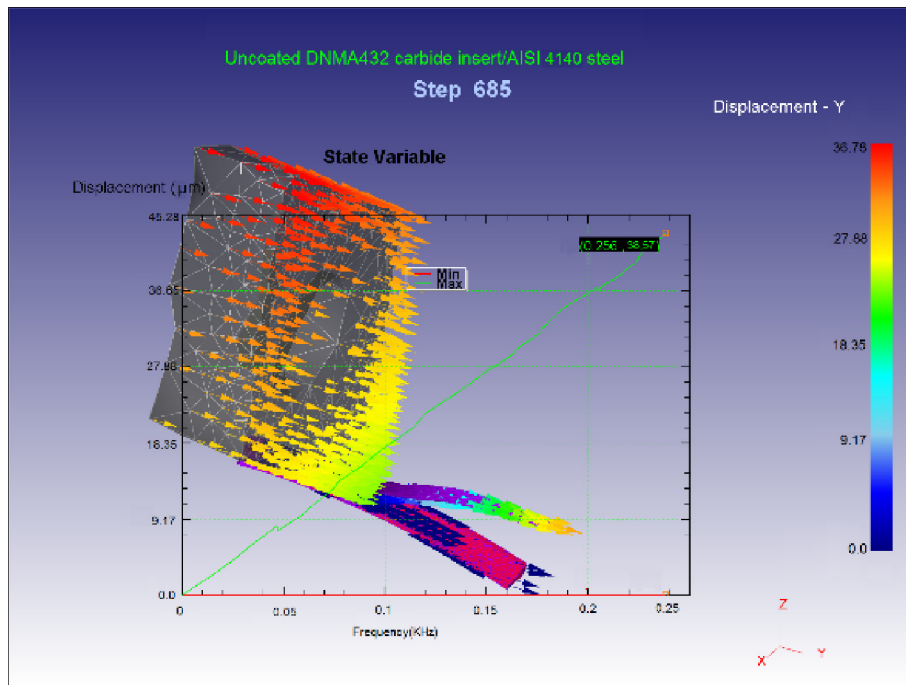


Fig. 6. Uncoated DNMA 432/AISI 4140.

6(c) FE predicted load in feed direction

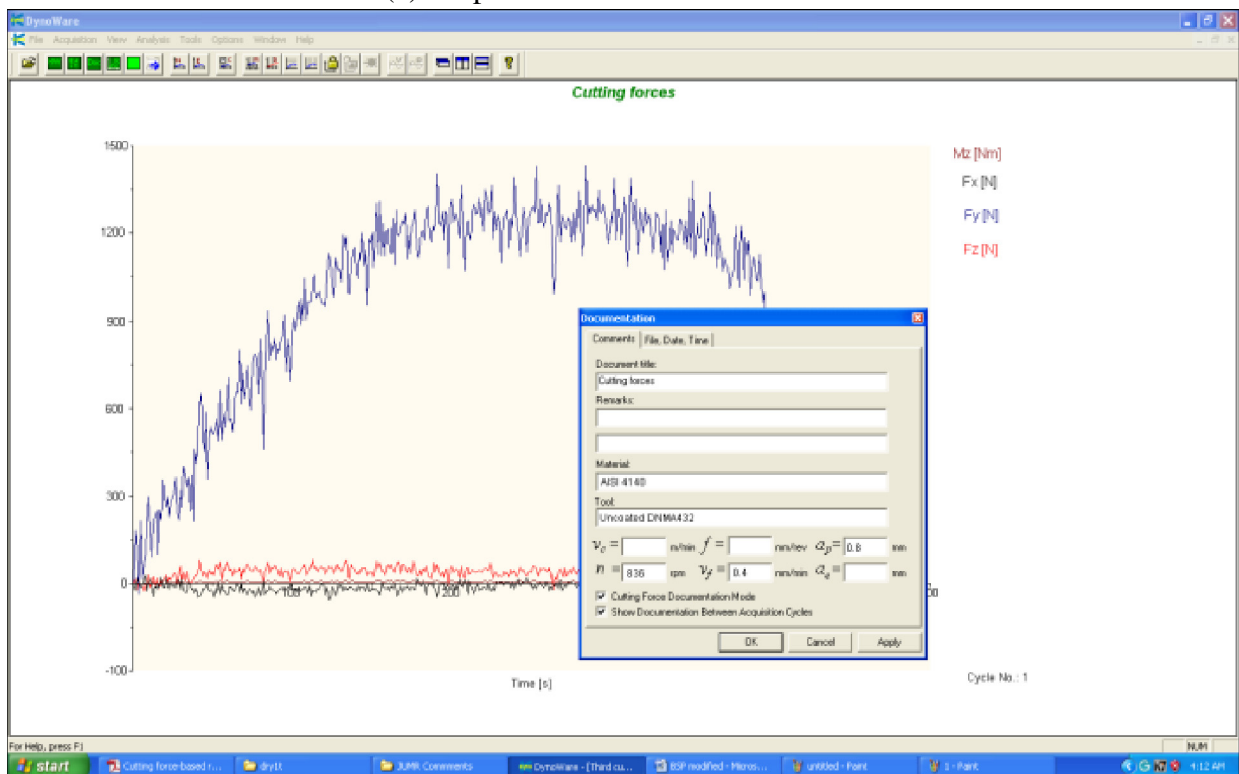


Fig. 6 (continued)

show the relationship between FE simulation values with experimental or measured values [45]. Fig. 6(a) gives numerical displacement (36.78 μm) whereas measured displacement is found to be

(35 μm) in TC1-1 is shown in Fig. 6(b). Fig. 6(c) shows the numerically predicted load in the feed direction (625 N) compared with measured force, F_y (600 N) presented in Fig. 6(d) for test condition

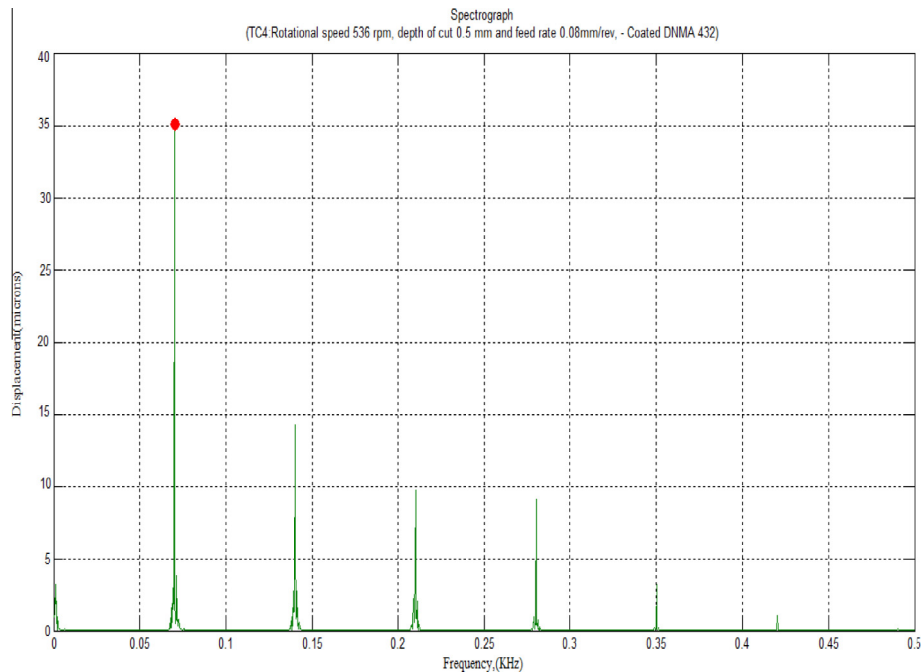


Fig. 6 (continued)

T: 2-5 Rotational speed 836 rpm, feed at 0.4 mm/rev, depth of cut 0.8 mm

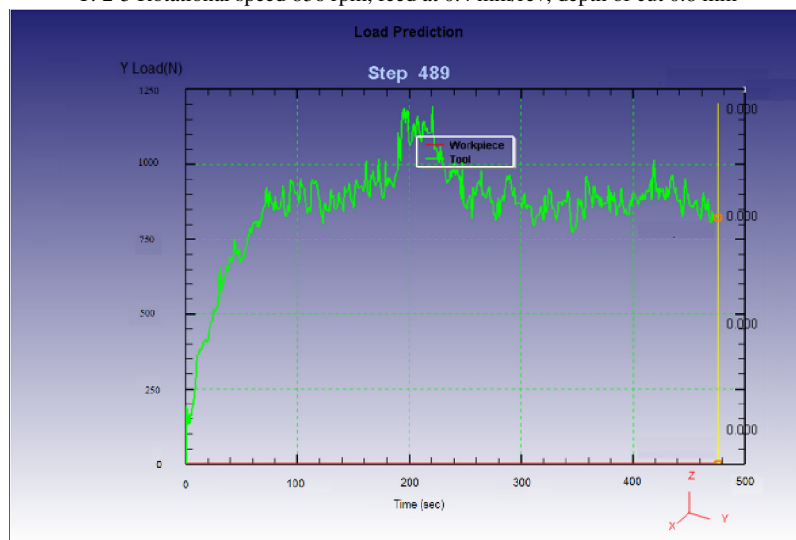


Fig. 6 (continued)

TC2-8. In Fig. 6(e), the flank wear profile predicted in 3D FE simulation is compared with measured tool wear profile, with OptoMech vision inspection system and presented in Fig. 6(f) for test condition TC3-9. It is true that simulated cutting time is very short (few milliseconds), this is sufficient to highlight wear localization zones and the intense thermo-mechanical loading at the contact interface leading to observed wear types [46]. The qualitative prediction of the tool wear corresponds closely to that observed by vision inspection method, as shown in Fig. 6(f). There is a close correspondence between FE prediction and OptoMech vision observation of the tool wear at the flank face. The error between the results varies between 5 and 9% throughout the experiment. FE simulations were generated [47] for uncoated cutting insert and AISI 4140 as workpiece material.

4. Development of empirical relationship displacement amplitude and tool flank wear

In the present work, vibration displacement ($Disp$) and tool wear (VB) are selected as the response variables. Feed rate (f), spindle speed (s), depth of cut (d) at different levels of workpiece hardness (H) are the machining parameters. The machinability performance of displacement amplitude (μm) and tool wear (mm) are obtained, to analyze the machining parameters with the help of [48,49] response surface methodology (RSM). The relationship of preferred response and independent variables for input are represented in the appropriate form as follows. Feed rate, cutting speed, depth of cut, different hardness levels (independent variables) which vary during the experiments. For each factor,

TC:3-9: Rotational speed 1135 rpm, feed at 0.8 mm/rev, depth of cut 1.2 mm

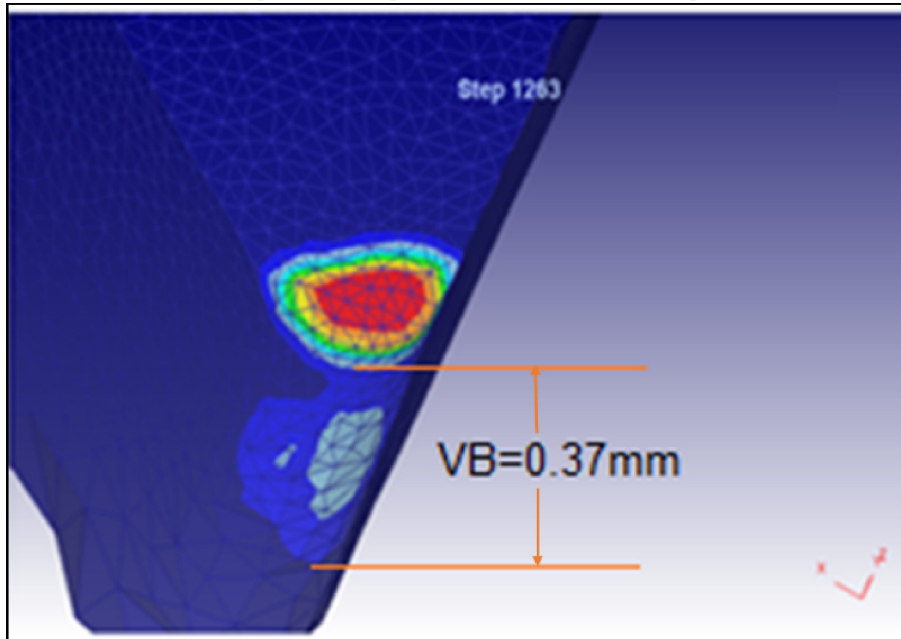


Fig. 6 (continued)

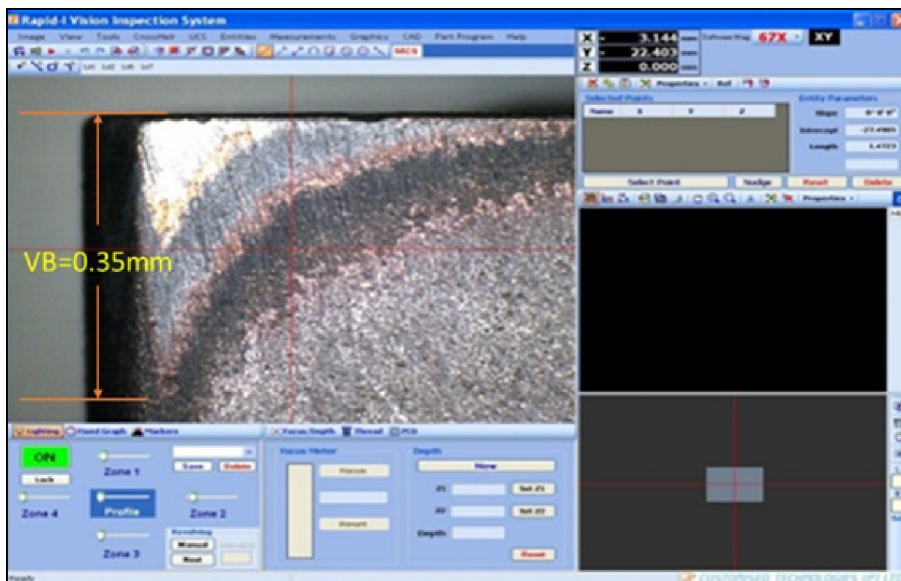


Fig. 6 (continued)

three stages are deliberately chosen and set during the experimentation according to the DOE. The response surface methodology (RSM) is also employed. Box-Behnken design is used to identify the cause and effect of the relationship between the control variables and the responses. Therefore, the degree of freedom model for vibration displacement prediction in their investigation of the conformity between workpiece and cutting tool in turning process.

The variation in displacement amplitude and corresponding tool wear with machining parameters (input parameters N , f , d , H) are being mathematically developed using the regression analysis method. Eq. (5) ($Disp_{num}$) represents the numerical displacement data whereas Eq. (6) represents (VB_{num}) the numerically predicted tool flank wear data. Table 3 gives both experimental and numerical results.

To obtain scientific understandings of work materials and process variables effects on the tooling performance. A numerical simulation model is evaluated based on experimental research, and subsequent mathematical models have developed for different cases. The mathematical modeling did by polynomial equations that are very helpful in comparing the relationship between the process variables using minitab software. In turning, displacement ($Disp$) due to vibration is expressed as a function of the process parameters and workpiece hardness as shown in Eq. (2).

$$Disp = f(N, f, d, H) \quad (2)$$

where $Disp$ – machining response, f – response function and the turning process variables such as s , f , d , H . In the analysis, a procedure for an approximation of response is derived using the built-in

Table 3
Experimental and numerical results at different test conditions.

Test condition	Cutting speed (<i>N</i>)	Feed rate (<i>f</i>)	Depth of cut (<i>d</i>)	Hard-ness (<i>H</i>)	Displacement, <i>Disp</i> (μm)		Flank wear, VB (mm)	
					Experimental	FE predicted	Experimental	FE predicted
TC 1-1	538	0.08	0.5	152.5	12	11.60	0.08	0.074
TC 1-2	538	0.08	0.8	153.5	14	13.88	0.10	0.092
TC 1-3	538	0.08	1.5	155.5	16	15.80	0.12	0.1260
TC 1-4	538	0.4	0.5	157	18	17.56	0.14	0.1288
TC 1-5	538	0.4	0.8	158.5	21	20.05	0.17	0.1685
TC 1-6	538	0.4	1.5	160	26	24.92	0.19	0.1748
TC 1-7	538	0.8	0.5	161.5	28	27.40	0.2	0.197
TC 1-8	538	0.8	0.8	164	30	29.60	0.24	0.228
TC 1-9	538	0.8	1.5	167	32	31.60	0.26	0.263
TC 2-1	836	0.08	0.5	153.5	16	15.72	0.15	0.138
TC 2-2	836	0.08	0.8	153	20	19.69	0.15	0.145
TC 2-3	836	0.08	1.5	155	22	21.24	0.17	0.164
TC 2-4	836	0.4	0.5	157	24	23.20	0.21	0.205
TC 2-5	836	0.4	0.8	158.5	32	30.44	0.26	0.249
TC 2-6	836	0.4	1.5	160	42	41.25	0.31	0.305
TC 2-7	836	0.8	0.5	162	50	47.50	0.32	0.314
TC 2-8	836	0.8	0.8	164	60	58.58	0.32	0.319
TC 2-9	836	0.8	1.5	169	72	70.24	0.33	0.320
TC 3-1	1135	0.8	0.5	155	12	11.71	0.21	0.209
TC 3-2	1135	0.8	0.8	158	16	14.72	0.24	0.225
TC 3-3	1135	0.8	1.5	159	22	21.10	0.26	0.262
TC 3-4	1135	0.4	0.5	162	26	24.92	0.36	0.332
TC 3-5	1135	0.4	0.8	164	38	37.90	0.39	0.395
TC 3-6	1135	0.4	1.5	165	48	47.16	0.41	0.392
TC 3-7	1135	0.8	0.5	168	60	58.55	0.43	0.428
TC 3-8	1135	0.8	0.8	170	72	70.24	0.46	0.453
TC 3-9	1135	0.8	1.5	173	84	83.20	0.49	0.485

2nd order polynomial regression as the quadratic model. The quadratic model for machining response as mentioned below. The second-order polynomial (regression) equation used to represent the response surface for displacement amplitude (*Disp*) is given by:

$$Disp = b_0 + \sum b_i X_i + \sum b_{ii} X_i^2 + \sum b_{ij} X_i X_j \tag{3}$$

and for four factors, the selected polynomial can be expressed as:

$$Disp = b_0 + b_1 N + b_2 f + b_3 d + b_4 H + b_{12} Nf + b_{13} Nd + b_{14} NH + b_{23} fd + b_{24} fH + b_{34} dH + b_{11} N^2 + b_{22} f^2 + b_{33} d^2 + b_{44} H^2 \tag{4}$$

where $b_1, b_2, b_3, \dots, b_{44}$ are regression coefficients [25] and b_0 is the average of the output responses. These coefficients depend on the respective linear, interaction, and squared terms of factors. The

value of the coefficient was calculated using minitab software. Significance of each factor determined by 'p' values, which are presented in Tables 4–7. For the values of 'p' less than 0.05, indicate that the model terms are significant. In this case, $X_1, X_2, X_4, X_{12}, X_{22}$ and X_1, X_2 are significant model terms and X_3 has less influence on the displacement. The values greater than 0.10 indicate that the model terms are not significant. The final empirical relationship is constructed using only these coefficients and developed the empirical relationship given below.

$$Disp_{num} = 43.92 + 4.8N + 2.11f + 2.36d + 26.1H - 20.22N^2 + 8.1f^2 - 1.24d^2 + 13.54H^2 - 6.1(N \cdot f) - 3.22(N \cdot d) + 32.28(N \cdot H) + 2.10(f \cdot d) - 22.78(f \cdot H) - 1.12(d \cdot H) \tag{5}$$

Table 4
ANOVA table for experimental displacement.

Source	DF	Seq SS	Adj SS	Adj MS	F	P	Remarks
<i>N</i>	1	1839.1	1.4	1.38	0.13	0.010	S
<i>f</i>	1	2100.4	2.9	2.88	0.28	0.606	NS
<i>d</i>	1	716.2	0.2	0.24	0.02	0.035	S
<i>H</i>	1	4198.5	63.1	63.13	6.16	0.002	S
<i>N * N</i>	1	874.2	462.1	462.14	45.08	0.007	S
<i>f * f</i>	1	163.0	24.7	24.68	2.41	0.147	NS
<i>d * d</i>	1	1.0	6.0	6.04	0.59	0.021	S
<i>H * H</i>	1	159.1	4.8	4.80	0.47	0.039	S
<i>N * f</i>	1	372.0	0.7	0.66	0.06	0.804	NS
<i>N * d</i>	1	122.3	0.0	0.05	0.00	0.946	NS
<i>N * H</i>	1	73.5	27.5	27.47	2.68	0.128	NS
<i>f * d</i>	1	18.0	0.0	0.00	0.00	0.992	NS
<i>f * H</i>	1	45.2	13.5	13.48	1.32	0.274	NS
<i>d * H</i>	1	0.0	0.0	0.03	0.00	0.958	NS
Error	12	123.0	123	10.25	-	-	-
Total	26	-	-	-	-	-	-

R^2 value for the above table = 0.986.

Note: *N* = speed, *f* = feed, *d* = depth of cut, *H* = hardness, DF = degree of freedom, SS = sum of squares, MS = mean squares, S = significant, NS = not significant.

Table 5
ANOVA table for numerical displacement.

Source	DF	Seq SS	Adj SS	Adj MS	F	P	Remarks
<i>N</i>	1	1798.8	16.0	16.50	0.89	0.024	S
<i>F</i>	1	2102.7	0.55	0.42	0.02	0.625	NS
<i>D</i>	1	699.5	5.9	5.72	0.13	0.007	S
<i>H</i>	1	4021.5	28.4	28.13	1.27	0.003	S
<i>N * N</i>	1	709.6	460.2	470.19	23.62	0.036	S
<i>f * f</i>	1	169.3	24.3	25.73	1.26	0.263	NS
<i>d * d</i>	1	0.01	5.2	5.05	0.22	0.048	S
<i>H * H</i>	1	192.7	10.8	10.10	0.44	0.044	S
<i>N * f</i>	1	368.2	11.3	11.35	0.55	0.432	NS
<i>N * d</i>	1	126.1	15.5	15.16	0.78	0.368	NS
<i>N * H</i>	1	131.4	81.1	87.71	3.42	0.042	S
<i>f * d</i>	1	1.1	4.3	4.90	0.25	0.610	NS
<i>f * H</i>	1	41.2	18.3	18.17	1.01	0.336	NS
<i>d * H</i>	1	0.5	0.55	0.52	0.02	0.867	NS
Error	12	217.1	207.7	17.29	-	-	-
Total	26	-	-	-	-	-	-

R^2 value for the above table = 0.978.

Note: *N* = speed, *f* = feed, *d* = depth of cut, *H* = hardness, DF = degree of freedom, SS = sum of squares, MS = mean squares, S = significant, NS = not significant.

Table 6
ANOVA table for experimental tool wear.

Source	DF	Seq SS	Adj SS	Adj MS	F	P	Remarks
N	1	938.97	0.22	0.224	0.02	0.001	S
f	1	1582.59	1.59	1.589	0.13	0.027	S
d	1	438.04	0.38	0.376	0.03	0.015	S
H	1	2745.66	40.45	40.447	3.25	0.021	S
N * N	1	144.43	133.02	133.021	10.69	0.013	S
f * f	1	138.69	19.53	19.529	1.57	0.020	S
d * d	1	1.02	2.00	2.001	0.16	0.002	S
H * H	1	86.08	7.86	7.860	0.63	0.009	S
N * f	1	141.92	0.22	0.217	0.02	0.897	NS
N * d	1	53.92	0.74	0.741	0.6	0.811	NS
N * H	1	24.25	17.17	17.165	1.38	0.263	NS
f * d	1	0.00	6.30	6.304	0.51	0.044	S
f * H	1	10.77	10.86	10.864	0.87	0.369	NS
d * H	1	3.03	3.03	3.032	0.24	0.631	NS
Error	12	149.37	149.37	12.447	-	-	-
Total	26	-	-	-	-	-	-

R² value for the above table = 0.9769.

Note: N = speed, f = feed, d = depth of cut, H = hardness, DF = degree of freedom, SS = sum of squares, MS = mean squares, S = significant, NS = not significant.

Table 7
ANOVA table for numerical tool wear data.

Source	DF	Seq SS	Adj SS	Adj MS	F	P	Remarks
N	1	927.85	9.58	9.578	0.45	0.008	S
f	1	1651.1	0.39	0.32	0.02	0.020	S
D	1	439.36	0.73	0.729	0.03	0.018	S
H	1	2565.28	19.84	19.840	0.93	0.022	S
N * N	1	102.34	178.46	178.459	8.33	0.001	S
f * f	1	165.97	34.03	34.026	1.59	0.002	S
d * d	1	0.27	0.44	0.436	0.02	0.039	S
H * H	1	141.1	31.14	31.141	1.45	0.009	S
N * f	1	131.92	30.46	30.460	1.42	0.256	NS
N * d	1	51.56	28.15	28.149	1.31	0.274	NS
N * H	1	78.23	81.81	81.812	3.82	0.074	NS
f * d	1	14.0	40.82	40.822	1.91	0.022	S
f * H	1	15.13	30.23	30.230	1.41	0.258	NS
d * H	1	15.98	15.8	15.978	0.75	0.405	NS
Error	12	257.09	257.09	21.424	-	-	-
Total	26	-	-	-	-	-	-

R² value for the above table = 0.9608.

Note: N = speed, f = feed, d = depth of cut, H = hardness, DF = degree of freedom, SS = sum of squares, MS = mean squares, S = significant, NS = not significant.

Table 8
Regression coefficients of each model.

Parameter	Regression coefficient		Model
	R ²		
	Experimental	Numerical	
Displacement	0.986	0.978	2nd order RSM
Tool wear	0.976	0.960	2nd order RSM

As shown in Eqs. (5) and (6), a similar mathematical modeling is carried for flank wear and displacement data also. Coefficients shown in ANOVA Tables 6 and 7 are used to develop empirical relationships for both the experimental and predicted flank wear data. The final empirical relationship is constructed using coefficients by Eq. (2), and the developed final empirical relationship is as follows:

$$\begin{aligned}
 VB_{num} = & 0.267 + 0.09N + 0.02f + 0.011d + 0.054H - 0.03N^2 \\
 & + 0.021f^2 - 0.002d^2 + 0.06H^2 - 0.058(N \cdot f) \\
 & - 0.025(N \cdot d) + 0.201(N \cdot H) + 0.0225(f \cdot d) \\
 & - 0.109(f \cdot H) - 0.026(d \cdot H)
 \end{aligned} \tag{6}$$

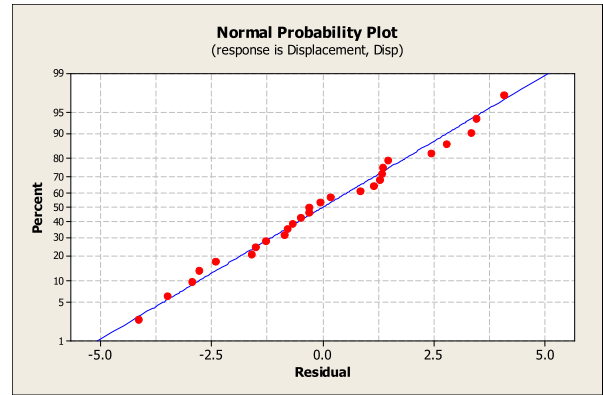


Fig. 7. (a) Normal probability plot for displacement ($Disp_{exp}$)-experimental data. (b) Normal probability plot for displacement ($Disp_{pre}$)-numerical data.

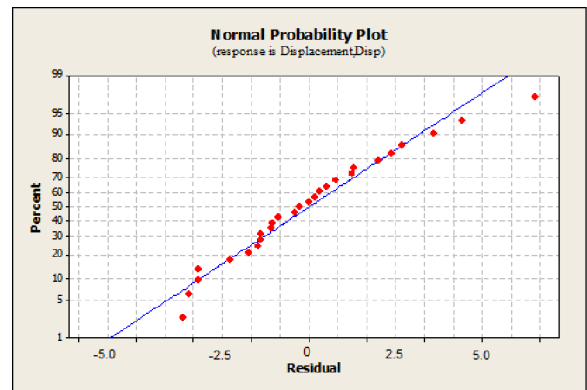


Fig. 7 (continued)

After obtaining the predicted values, these equations are used to correlate each other. The ANOVA tables for flank wear shown in the Tables 7 and 8. Results in the tables clearly identify the significant factors that affect the tool wear in both experimental data and predicted data. These equations will give the expected values of displacement amplitude and flank wear for any combination of factor levels given that the levels are within the ranges stated in Table 1. From the above equations, it can be concluded that equations are approximately similar (3) & (4) and (5) & (6) to each other. Displacement amplitude and tool wear influenced by the factors on the right-hand side in both the cases. The above mathematical model can be used to predict the values of the displacement, and flank wear of the factors studied.

5. Results and discussions

The design of experiments technique determines the optimum number of trails required for experimentation. To evaluate the influence of cutting speed, feed, the depth of cut and workpiece hardness on the response variables, an ANOVA is carried out. The normal probability plots for experimental displacement amplitude shown in Fig. 7(a), and Fig. 7(b) gives the FE predicted data. The adequacy of the model has been being investigated by the examination of residuals. The residuals, which are the difference between the respective observed response and the predicted response, are examined using normal probability plots of the residuals and the plots of the residuals versus the predicted response. If the model is adequate, the points on the normal probability plots of the residuals should form a straight line. On the other hand,

the plots of the residuals versus the predicted response should observe less, that is, they should contain no distinct pattern. If the residuals plot approximately along a straight line, then the normality assumption is satisfied. In this study, the residuals can be judged as normally distributed; achieving normality assumptions for both of the responses. Fig. 7(a) and (b) show the normal probability plots of the residuals and the plots of the residuals versus the predicted response for the surface roughness values. It reveals that the residuals fell on a straight line implying that the distribution of errors is normal. Fig. 7(a) and (b), reveal that there is no defined pattern and unusual structure. This shows that the model proposed is adequate, and there is no reason to suspect any violation of the independence or constant variance assumption [48]. This analysis allows verifying the normal distribution of residuals (Fig. 7(a) (b)) to test the normality of experimental data, and, if necessary, to identify the correct representations of the experimental values for obtaining normal distributions of residuals and pass the normality tests. The analysis is carried out for a level of significance of 5%, so for a level of confidence of 95%. The probability plot is used to determine if a normal distribution fits the collected data.

Surface charts presented in Fig. 8 which shows a three-dimensional surface that connects a set of data points ($Disp$ vs. d , N ; $disp$ vs. d , f). Fig. 8(a) shows the relationship between the depth of cut and cutting speed with displacement amplitude whereas Fig. 8(b) presents the relationship between the depth of cut and feed rate with displacement amplitude in the workpiece for cutting condition. It observed that an increase in the displacement of the

workpiece is due to increase in the level of workpiece hardness which increases tool wear.

Similarly, Fig. 9(a) and (b), it is summarized that the tool flank wear values are within the control range, indicating that there is no correct pattern and unusual structure. The residual analysis does not indicate any model inadequacy. Hence, these values yield better results in future predictions. It satisfies the conditions of the normal distribution curve, which is reliable.

Surface plots presented in Fig. 10(a) and (b) shows the effect of feed rate, depth of cut and workpiece hardness on the tool wear in both experimental and simulated cases. Fig. 10(a) and (b) holds the same interpretation for flank wear (VB) values for FE simulation results. These surface plots used to set up an agreement between cutting parameters and output process variables for machining cutting combinations. It shows that the cutting tool wear is directly proportional to the workpiece displacement.

Surface plots are constructed to illustrate the consequences of induced vibration amplitude due to the effect of feed rate, cutting speed, and depth of cut. It is clear that the increase in displacement amplitude during the machining have a significant effect on tool wear. From the experimental results the vibrations increase with increasing the cutting speed. ANOVA is performed for regression analysis and is presented in Tables 4–7. The p -value in every table indicates that the estimated model (Tables 4 and 6) by regression analysis is significant at the α -level of 0.05. This value implies that at least one coefficient is different from zero [25]. By observing the p -value column of ANOVA Tables 4–7, it is possible to state that the

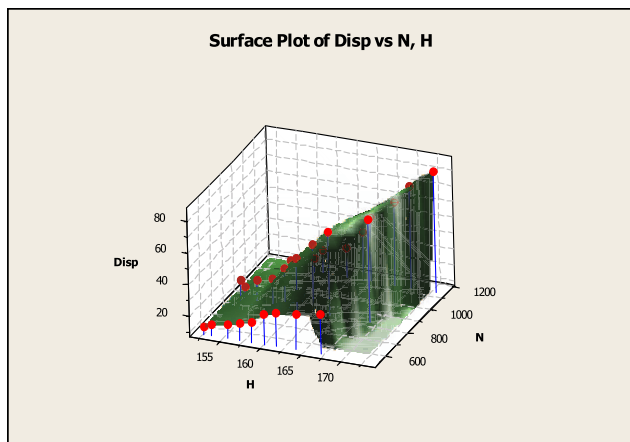


Fig. 8. (a) Surface plots of displacement ($Disp_{exp}$)-experimental data. (b) Surface plots of displacement ($Disp_{num}$)-numerical data.

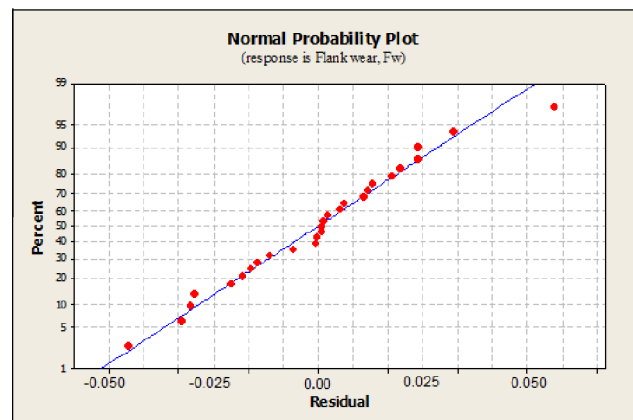


Fig. 9. (a) Normal probability plot for tool wear (VB_{exp})-experimental data. (b) Normal probability plot for tool wear (VB_{pre})-numerical data.

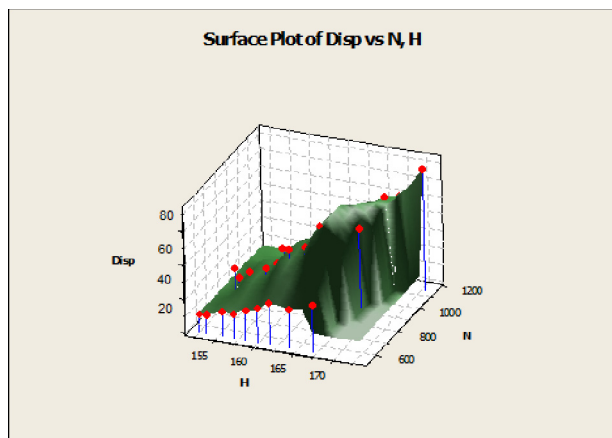


Fig. 8 (continued)

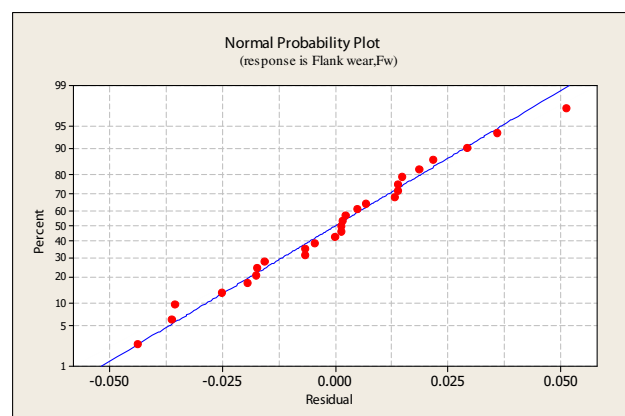


Fig. 9 (continued)

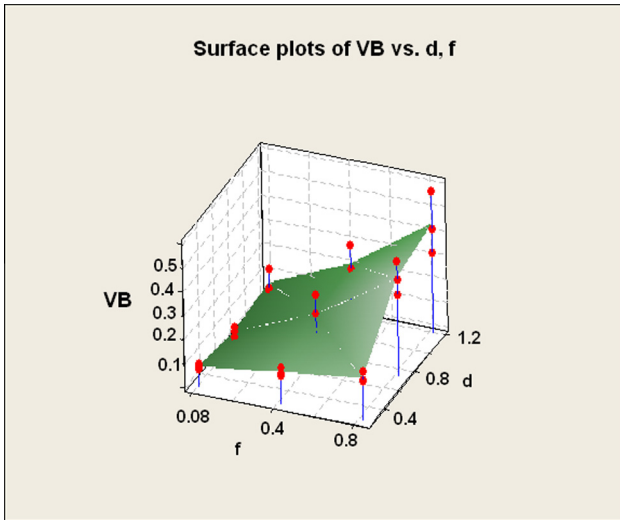


Fig. 10. (a) Surface plots of tool wear (VB_{exp})-experimental data. (b) Surface plots of tool wear (VB_{num})-numerical data.

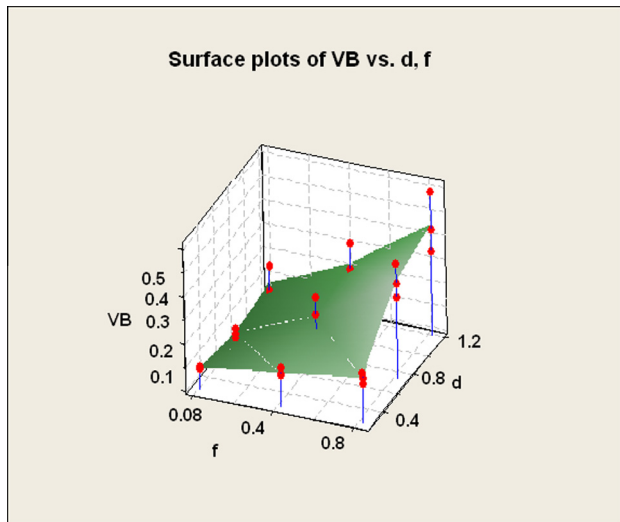


Fig. 10 (continued)

hardness of workpiece and feed rate shows relatively less influence on the evolution of displacement amplitude and tool wear. The diagnostic checking is done through residual analysis for the developed model. Residuals falling in a straight line shows that the errors are normally distributed. Tables 4 and 5 shows the verification of the predicted test results of vibration displacement. The predicted machining parameters' performance compared with the actual machining performance and a good agreement identified between these performances. The above mathematical models for displacement amplitude and tool wear are of importance in the selection of machining parameters during the machining of the cylindrical parts. The ANOVA table for experimental displacement shown in Table 4 and for numerical displacement is presented in Table 5.

From the results Tables 4 and 5, it can be concluded that the displacement factor is influenced by the cutting speed and the workpiece hardness values. The R -Square values for experimental and simulated methods are 98.6 and 97.8 respectively, which indicates that simulated values shows good agreement with the experimental values that are helpful in estimating displacement amplitude.

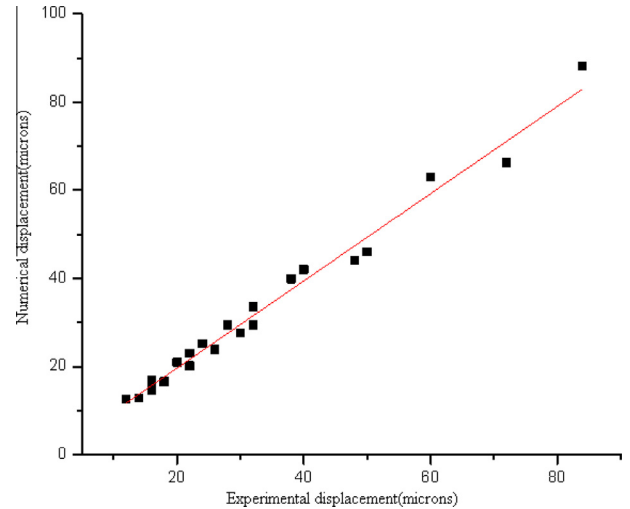


Fig. 11. (a) Vibration displacement. (b) Flank wear.

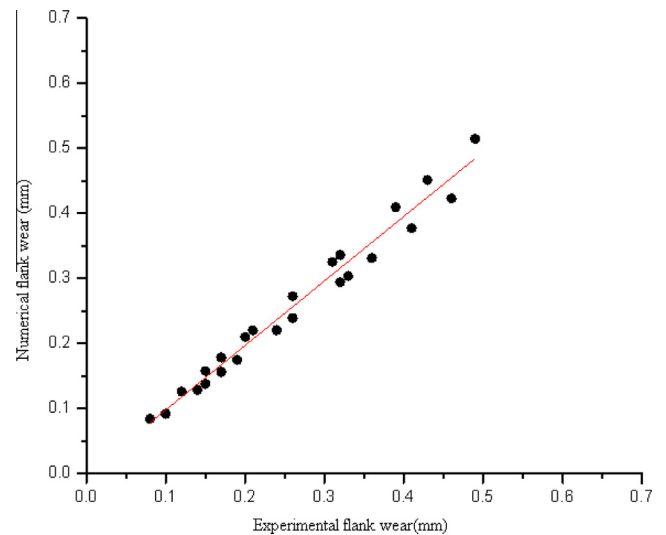


Fig. 11 (continued)

Table 6 gives the ANOVA verification results of experimental flank wear and Table 7 shows the ANOVA data of FE simulated flank wear. From the results, it is concluded that the tool wear is more influenced by the cutting speed, feed rate, workpiece hardness and depth of cut values as well. The R -Square values for experimental and simulated methods are 97.69 and 96.08 respectively, which indicates that simulated values are in close relation with the experimental values that are helpful in estimating the tool wear.

In the present work, an attempt is made to use the data from vibration signals in predicting tool wear using response surface methodology [49]. Fig. 11 shows the comparison graph from which the closeness of experimental values and predicted values observed in the study. Fig. 11(a) gives the agreement between experimental and numerically predicted displacements values and Fig. 11(b) presents the closeness between the experimental and numerically predicted flank wear values. The results of the comparison are proven to predict the values of displacement amplitude, and flank wear close to the readings recorded experimentally with a 95% confidence interval that indicates a good agreement with the results.

6. Validation of the model

Forecasting ability of the two polynomial models, i.e. Eqs. (5) and (6), it is clear that the best results provided by the 2nd order polynomial function. These results confirm the estimation of regression coefficients of each reported in Table 8.

7. Conclusions

In present work performance of uncoated carbide tool is evaluated by considering the cutting parameters and different levels in work material hardness during turning of AISI 4140 steel. Multiple linear regression models were developed to establish the correlations between the cutting parameters and performance measures like displacement amplitude and tool life. The coefficient of regression is found to be near to 0.9, indicates that the developed models are highly reliable and could be used effectively for predicting the responses within the domain of the cutting parameters. ANOVA determines the highly significant parameters. Experimental observations show that values of displacement amplitude are found to be increasing along with workpiece hardness level, depth of cut and rotational speed. A similar trend is observed in tool wear as well. Optimum cutting conditions are determined using response surface methodology (RSM) and the desirability function approach. The results have indicated that the effect of feed rate and depth of cut at different levels workpiece hardness is more when tool wear is the on the desired parameter. When the desired parameter is displacement, then the effect of rotational speed along with different levels of workpiece hardness is found to be more significant. Both displacement amplitude and flank wear highly affected by factors considered in the study. Results show a relatively good agreement between prediction and experimental values through empirical models developed.

References

- [1] Doug Roberts, Precision Microdrives Tech Blog, <<http://www.precisionmicrodrives.com/tech-blog/2013/02/25/why-is-vibration-amplitude-in-g>> 2013.
- [2] M. Siddhpura, R. Paurobally, A review of chatter vibration research in turning, *Int. J. Mach. Tools Manuf.* 61 (2012) 27–47.
- [3] I. Claesson, L. Håkansson, Adaptive active control of machine-tool vibration in a lathe, *Int. J. Acoust. Vib.* 3 (4) (1998) 155–161.
- [4] P. Sam Paul, A.S. Varadarajan, R. Robinson Gnanadurai, Study on the influence of fluid application parameters on tool vibration and cutting performance during turning of hardened steel, *Eng. Sci. Technol. Int. J.* 19 (2016) 241–253.
- [5] Guillem Quintana, Joaquim Ciurana, Chatter in machining processes: a review, *Int. J. Mach. Tools Manuf.* 51 (2011) 363–376.
- [6] L. Zhou, S.J. Chen, K. Cheng, Identification of tool-workpiece relative vibration in diamond turning by areal power spectral density, *Nanotechnol. Precis. Eng.* 8 (2) (2010) 137–142.
- [7] B.E. Clancy, Y.C. Shin, A comprehensive chatter prediction model for face turning operation including tool wear effect, *Int. J. Mach. Tools Manuf.* 42 (2002) 1035–1044.
- [8] N. Deshpande, M.S. Fofana, Non-linear regenerative chatter in turning, *Robot. Comput. Integr. Manuf.* 17 (1–2) (2001) 107–112.
- [9] L. Carrino, G. Giorleo, W. Polini, U. Prisco, Dimensional errors in longitudinal turning based on the unified generalized mechanics of cutting approach part II: three-dimensional theory, *Int. J. Mach. Tools Manuf.* 42 (14) (2002) 1509–1515.
- [10] Ch. Shoba, N. Ramanaiah, D. Nageswara Rao, Effect of reinforcement on the cutting forces while machining metal matrix composites – an experimental approach, *Eng. Sci. Technol. Int. J.* 18 (2015) 658–663.
- [11] D.R.H. Jones, Whirling failure in a woodworking lathe, *Eng. Fail. Anal.* 3 (1) (1996) 71–76.
- [12] S. Jayakumar, K. Marimuthu, T. Ramachandran, Prediction of vibration amplitude and surface roughness in machining of Al6061 metal matrix composites by response surface methodology, *Int. J. Mech. Mater. Eng.* 7 (3) (2013) 222–231.
- [13] Y. Sahin, A.R. Motorcu, Surface roughness model for machining mild steel with coated carbide tool, *Mater. Des.* 26 (4) (2005) 321–326.
- [14] M. Barkallah, J. Louati, M. Haddar, Evaluation of manufacturing tolerance using a statistical method and experimentation, *Int. J. Simul. Model.* 11 (2012) 5–16.
- [15] M. Siddhpura, R. Paurobally, Experimental investigation of chatter vibrations in facing and turning processes, *World Acad. Sci. Eng. Technol.* 7 (2013) 84–89.
- [16] P.J. Arrazola, T. Özel, D. Umbrello, M. Davies, I.S. Jawahir, Recent advances in modeling of metal machining processes, *CIRP Ann. Manuf. Technol.* 62 (2) (2013) 695–718.
- [17] Claudiu F. Bisu, Philippe Darnis, Alain Gérard, Jean-Yves Knevez, Displacements analysis of self-excited vibrations in turning, *Int. J. Adv. Manuf. Technol.* 44 (2008) 1–16.
- [18] Aco Antić, Dražan Kozak, Borut Kosec, Goran Simunovic, Timislav Saric, Dusan Kovacevic, Robert Cep, Influence of tool wear on the chip-forming mechanism and tool vibrations, *Mater. Technol.* 46 (3) (2012) 279–285.
- [19] Aco Antić, Goran Simunovic, Timislav Saric, Mijodrag Milosevic, Mirko Ficko, A model for tool wear monitoring system for turning, *Strojnikivestnik J. Mech. Eng.* 52 (11) (2006) 763–776.
- [20] Jan C. Aurich, Marco Zimmermann, Stefan Schindler, Paul Steinmann, Analysis of the machining accuracy when dry turning via experiments and finite element simulations, *Prod. Eng. Res. Dev.* 8 (2014) 41–50.
- [21] B. Haddag, T. Kagnaya, M. Nouari, T. Cutard, A new heat transfer analysis in machining based on two steps of 3D finite element modelling and experimental validation, *Heat Mass Transf.* 49 (2013) 129–145.
- [22] B. Haddag, M. Nouari, Tool wear and heat transfer analyses in dry machining based on multi-steps numerical modelling and experimental validation, *Wear* 302 (1–2) (2013) 1158–1170.
- [23] Tuğrul Özel, Tsu-Kong Hsu, Erol Zeren, Effects of cutting edge geometry, workpiece hardness, feed rate and cutting speed on surface roughness and forces in finish turning of hardened AISI H13 steel, *Int. J. Adv. Manuf. Technol.* 25 (2005) 262–269.
- [24] Tuğrul Özel, Erol Zeren, Finite element modeling the influence of edge roundness on the stress and temperature fields induced by high-speed machining, *Int. J. Adv. Manuf. Technol.* 35 (2010) 255–267.
- [25] Fazar Akbar, Paul T. Mativenga, M.A. Sheikh, An experimental and coupled thermo-mechanical finite element study of heat partition effects in machining, *Int. J. Adv. Manuf. Technol.* 46 (2010) 491–507.
- [26] B. Haddag, M. Nouari, C. Barlier, J. Dhers, Experimental and numerical analyses of the tool wear in rough turning of large dimensions components of nuclear power plants, *Wear* 312 (2014) 40–50.
- [27] Tuğrul Özel, Yigit Karpat, Predictive modeling of surface roughness and tool wear in hard turning using regression and neural networks, *Int. J. Mach. Tools Manuf.* 45 (2005) 467–479.
- [28] R. Robinson Gnanadurai, A.S. Varadarajan, Investigation on the effect of cooling of the tool using heat pipe during hard turning with minimal fluid application, *Eng. Sci. Technol. Int. J.* (2016), <http://dx.doi.org/10.1016/j.jestch.2016.01.012>.
- [29] I. Mukherjee, P.K. Ray, A review of optimization techniques in metal cutting processes, *Comput. Ind. Eng.* 50 (2006) 15–34.
- [30] X. Feng, X. Wang, Development of empirical models for surface roughness prediction in finish turning, *Int. J. Adv. Manuf. Technol.* 20 (2002) 348–356.
- [31] Fang Shao, Liu Zhanqiang, Yi Wan, Zhenyu Shi, Finite element simulation of machining of Ti6Al4V alloy with thermodynamical constitutive equation, *Int. J. Adv. Manuf. Technol.* 49 (2010) 431–439.
- [32] R. Arokiadass, K. Palaniradja, N. Alagumoorathi, Prediction and optimization of end milling process parameters of cast aluminium based MMC, *Trans. Nonferrous Metals Soc. China* 22 (2012) 1568–1574.
- [33] R.K. Bhushan, Multi response optimization of Al alloy-SiC composite machining parameters for minimum tool wear and maximum metal removal rate, *ASME J. Manuf. Sci. Eng.* 135 (2) (2013) 021013.
- [34] H. Aouici, M.A. Yallese, A. Belbah, M.F. Ameer, M. Elbah, Experimental investigation of cutting parameters influence on surface roughness and cutting forces in hard turning of X38CrMoV5-1 with CBN tool, *Sadhana@ Indian Acad. Sci.* 38 (3) (2013) 429–445.
- [35] R. Suresh, S. Basavarajappa, G.L. Samuel, Predictive modeling of cutting forces and tool wear in hard turning using response surface methodology, international conference on modeling optimization and computing, *Procedia Eng.* 38 (2012) 73–81.
- [36] Avinash A. Thakre, Shashank Soni, Modeling of burr size in drilling of aluminum silicon carbide composites using response surface methodology, *Eng. Sci. Technol. Int. J.* (2016), <http://dx.doi.org/10.1016/j.jestch.2016.02.007>.
- [37] Ravindranadh Bobbili, V. Madhu, A.K. Gogia, Multi response optimization of wire-EDM process parameters of ballistic grade aluminium alloy, *Eng. Sci. Technol. Int. J.* 18 (2015) 720–726.
- [38] Shailesh Dewangan, Soumya Gangopadhyay, Chandan Kumar Biswas, Multi-response optimization of surface integrity characteristics of EDM process using grey-fuzzy logic-based hybrid approach, *Eng. Sci. Technol. Int. J.* 18 (2015) 361–368.
- [39] Feng Ding, Zhengjia He, Cutting tool wear monitoring for reliability analysis using proportional hazards model, *Int. J. Adv. Manuf. Technol.* 5 (2011) 565–574.
- [40] A.G. Mamalis, J. Kundrak, A. Markopoulos, D.E. Manalagos, On the finite modeling of high speed hard turning, *Int. J. Adv. Manuf. Technol.* 38 (2008) 441–446.
- [41] G.H. Lim, Tool-wear monitoring in machine turning, *J. Mater. Process. Technol.* 51 (1995) 25–36.
- [42] B. Haddag, H. Makich, M. Nouari, J. Dhers, Characterization and modelling of the rough turning process of large-scale parts: tribological behaviour and tool wear analyses, *Procedia CIRP* 31 (2015) 293–298.
- [43] Svetan Ratchev, Shulong, Wei Haung, Adib A. Becker, Machining simulation and system integration combining FE analysis and cutting mechanics modeling, *Int. J. Adv. Manuf. Technol.* 35 (2007) 55–65.

- [44] B. Haddag, H. Makich, M. Nouari, J. Dhers, Tribological behaviour and tool wear analyses in rough turning of large-scale parts of nuclear power plants using grooved coated insert, *Tribol. Int.* 80 (2014) 58–70.
- [45] E.O. Ezugwu, D.A. Fadare, J. Bonney, R.B. Da Silva, W.F. Sales, Modeling the correlation between cutting and process parameters in high-speed machining of Inconel 718 alloy using an artificial neural network, *Int. J. Mach. Tools Manuf.* 45 (2005) 1375–1385.
- [46] A. Attanasio, E. Ceretti, A. Fiorentino, C. Cappellini, C. Giardini, Investigation and FEM-based simulation of tool wear in turning operations with uncoated carbide tools, *Wear* 269 (2010) 344–350.
- [47] A. Attanasio, E. Ceretti, C. Giardini, C. Cappellini, Tool wear in cutting operations: experimental analysis and analytical models, *J. Manuf. Sci. Eng. Trans. ASME* 135 (5) (2013) 051012.
- [48] M.Y. Noordin, V.C. Venkatesh, S. Sharif, S. Elting, A. Abdullah, Application of response surface methodology in describing the performance of coated carbide tools when turning AISI, 1045 steel, *J. Mater. Process. Technol.* 145 (2004) 46–58.
- [49] Surinder Kumar, Meenu Gupta, Meenu Gupta, P.S. Satsangi, Multiple-response optimization of cutting forces in turning of UD-GFRP composite using Distance-Based Pareto Genetic Algorithm approach, *Eng. Sci. Technol. Int. J.* 18 (2015) 680–695.